# Radio Frequency Voltage Sampling at Cryogenic Temperatures

Kevin Reuer *

January 2, 2017

*Semester project, in the Trapped Ion Quantum Information Group of Prof. J. P. Home, Institute for Quantum Electronics, ETH Zurich, supervised by C. Zhang and M. Malinowski

**Abstract**

The aim of this thesis to design and characterize a sampling circuit including a Schottky diode that samples a radio frequency (RF) voltage by a DC voltage with a precision of $1 \cdot 10^{-5}$ at cryogenic temperature. This test circuit can then be used to set up a feedback loop which stabilizes the RF voltage. This then allows us to control the secular frequency (and thus the motional quantum state) of a charged particle in an ion trap more precisely. In the end, I achieved to implement and characterize one sampling circuit, that is a promising candidate for stabilizing the RF voltage with high enough precision.

# Contents

# 1 Introduction

Radio Frequency (RF) voltage is commonly used to confine atomic ions or other charged particles in ion traps [1]. Due to the Laplace's equation it is impossible to build a static direct current (DC) potential that is trapping in all directions [2, p. 5]. Therefore, in Paul traps one uses a static DC potential to trap in one direction and an oscillating RF potential for the other directions. Although at any instant of time, the RF potential always has anti-confining component along one direction, this direction of anti-confining is changing periodically. As a result, the RF potential forms a ponderomotive potential which confines the ions. Consequently, the ions' motion has two components: the weak motion at RF frequency, which is called micromotion, as well as the so-called secular motion, which has lower frequency and larger amplitude [2, p. 6].

The secular motion is driven by field inhomogeneities in the trapping potential [2, p. 6] and is very important to control the quantum states of the ions. The frequency of the secular motion is proportional to the RF voltage amplitude [1, p. 1].

For various reasons, the RF voltage amplitude in the ion trap, which in our case operates at cryogenic temperatures, is not stable but can be noisy at the $10^{-3}$ level [3]. The main reason for this is that the RF voltage is amplified by a helical resonator inside the cryostat. However, the properties of the resonator, such as amplification, resonance frequency and input impedance, depend on temperature and temperature is usually not stable inside the cryostat. For example, an atomic oven inside the cryostat will heat up the resonator during ion loading, and when more (less) rf power is coupled into the resonator due to better (worse) impedance matching, the temperature of resonator also rises (drops). Other sources for the variations are the RF signal generator itself and resistive losses [4].

Consequently, we need to set up a feedback loop to actively stabilize the RF voltages applied onto the trap, and sampling the RF voltage amplitude is a prerequisite for that. However, it is difficult to set up a fast feedback loop at cryogenic temperatures. Furthermore, one needs to be careful not to overload the resonator with the RF sampling circuit. A solution to this problem is to put a voltage divider in front of the probe, which protects the resonator from being overload, and then send the RF signal probe outside the cryostat and then into a feedback loop. However, this RF signal probe could inject noise into the RF input cable, thus effectively destabilizing the RF voltage on the trap.

A solution to this problem was found in [1]. One first converts the RF voltage probe into a DC voltage using a circuit including a diode. After that, one uses this DC signal to feedback and control the RF voltage. In [1] this resulted in a 34 dB reduction of trap frequency noise and drift. However, the setup in [1] operates at room temperature, not at cryogenic temperatures.

Thus, the aim of this thesis is to design and build a test circuit that samples RF voltage with a precision of $1 \cdot 10^{-5}$ at an RF voltage input of around 100 V at cryogenic temperatures by converting the RF amplitude into a DC voltage, which then can be measured at room temperature. For this, I first try to find a diode, which is cryo-compatible, integrate it into a sampling circuit and then measure its characteristics and stability both at room temperature and at cryogenic temperatures. The report will thus first mention general information on diode modelling and the diodes used, then describe the measurements done and the results obtained and finally analyze them in order to decide if the circuit designed and the diode used to sample the RF voltage faithfully and with sufficient precision.

# 2 Diodes

On this section, I first describe methods to model diodes and will give some information on the diodes used.

## 2.1 Diode modeling

To understand the circuit design, it is necessary to introduce two simple diode models and their response to an incident RF voltage: the piecewise linear model [5] and Shockley's equation [6]. The real voltage current characteristic of the diode is complicated and cannot be covered by a simple model (for realistic diode models see for example [7]). However, those easy models turn out to be sufficient to explain the functionality of the circuit, so I will limit myself to them. After discussing the diode models, I will briefly introduce the diodes used.

In the so-called piecewise linear model, as described in [5], one models a diode to be an ideal insulator below a certain voltage $v_d$ (therefore also for voltages applied in the reverse direction). Above this voltage $v_d$, the diode becomes conducting and behaves like an Ohmic resistance $R_d$ in series with a DC voltage source with voltage $v_d$. Fig. 1 shows the resulting voltage-current characteristic.

Since in the piecewise linear model, the diode is only conducting when the voltage across the diode $V$ is larger than $v_d$, it effectively cuts off the RF voltage and as a result the current through the diode looks like what is shown in Fig. 2. It is clear, that this current has a DC component, since the time averaged current will not be zero anymore. To make this even more obvious, Fig. 3 shows the fourier transform of the current through the diode. One recognizes that there is a large contribution at zero frequency which means that the current through the diode has a DC component.

Because the diode behaves like an Ohmic resistance for high RF voltages, $V_{RF} \gg v_d$, (see [8]), where $V_{RF}$ is the amplitude of the RF voltage (thus the voltage across the diode is $V = V_{RF}\sin(\omega t)$), as modeled in a piecewise linear model with $v_d \to 0$, the piecewise model is very accurate in this range. Therefore using the piecewise linear model and with the help of the approximation that $\frac{v_d}{V_{RF}} \to 0$, it follows for the DC component of the current through the diode

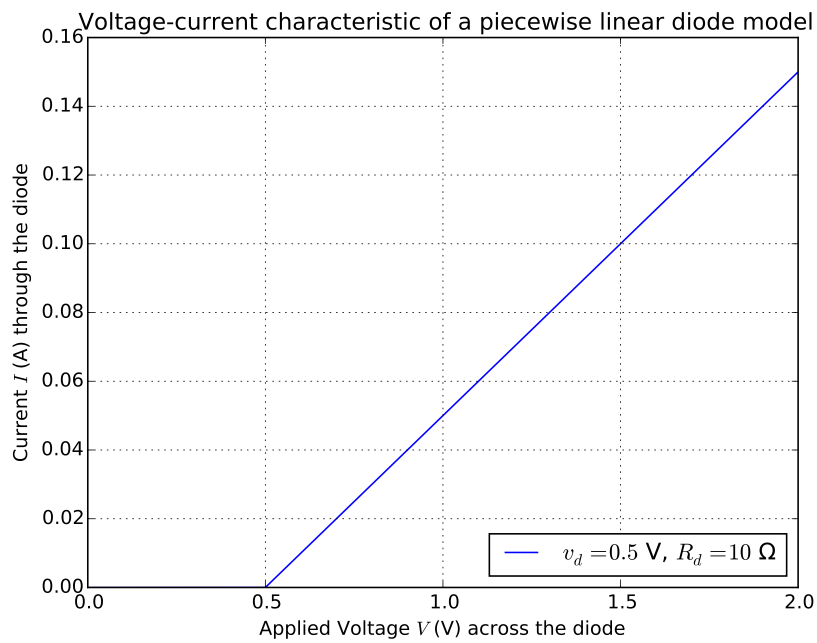


Figure 1: Voltage-current characteristic for a piecewise linear diode model with $v_d = 0.5$ V and $R_d = 10$ Ω.

$I_{out,DC}$:

$$I_{out,DC} \propto \int_0^{\frac{\pi}{\omega}} \frac{V_{RF}}{R_d} \cdot \sin(\omega t)\mathrm{d}t \tag{1}$$

$$\propto \frac{V_{RF}}{R_d} \tag{2}$$

where $\omega$ is the RF voltage angular frequency. Consequently, there is a linear dependence between the RF voltage amplitude $V_{RF}$ and the DC component of the through diode $I_{out,DC}$ for $V_{RF} \gg v_d$.

The second model, that is necessary to understand the measurement result, is the so called Shockley's equation, which describes the behavior of the diode for small voltages, both positive and negative (see [6]). Shockley's equation (derived by William Shockley in [9]) gives the current $I$ through the diode:

$$I = I_S \left( e^{\frac{V}{\eta V_t}} - 1 \right) \tag{3}$$

where $V$ is the voltage across the diode, $\eta$ is the so called emission factor (usually close to 1), $V_t = \frac{k_B T}{q}$ is the so called thermal voltage. which is around 25 mV for room temperature and around 0.35 mV at $T = 4$ K, $k_B$ is Boltzman's

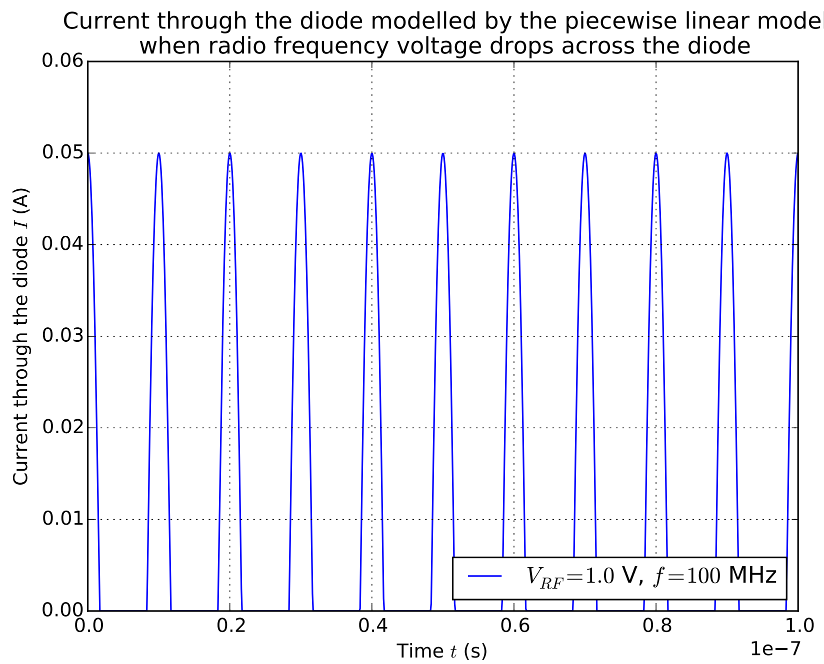


Figure 2: Current through the diode modelled by the piecewise linear model when radio frequency voltage with amplitude $V_{RF} = 1.0$ V and frequency $f = 100$ MHz drops across the diode.

constant, $T$ is the temperature, $q$ the electron charge, and $I_S$ the so called reverse saturation current. The voltage-current characteristics resulting from Shockley's equation is shown in Fig. 4.

The saturation current is strongly temperature dependent. The saturation current $I_S$ is [11]:

$$I_S = I_{SO} \left( \frac{T}{T_O} \right)^{\frac{2}{\eta}} e^{\frac{-q\psi}{k_B} \left( \frac{1}{T} - \frac{1}{T_O} \right)} \tag{4}$$

where $I_{SO}$ is the saturation current at 0 °C, $T$ is the absolute temperature, $\psi$ the metal-semiconductor Schottky barrier height and $T_O = 273$ K (0 °C). As a result, the saturation current decreases strongly when temperature drops.

If now an RF voltage is applied on the diode with $V = V_{RF} \cos(\omega t)$, where $\omega$ is the angular frequency of the RF voltage, I can insert this voltage into

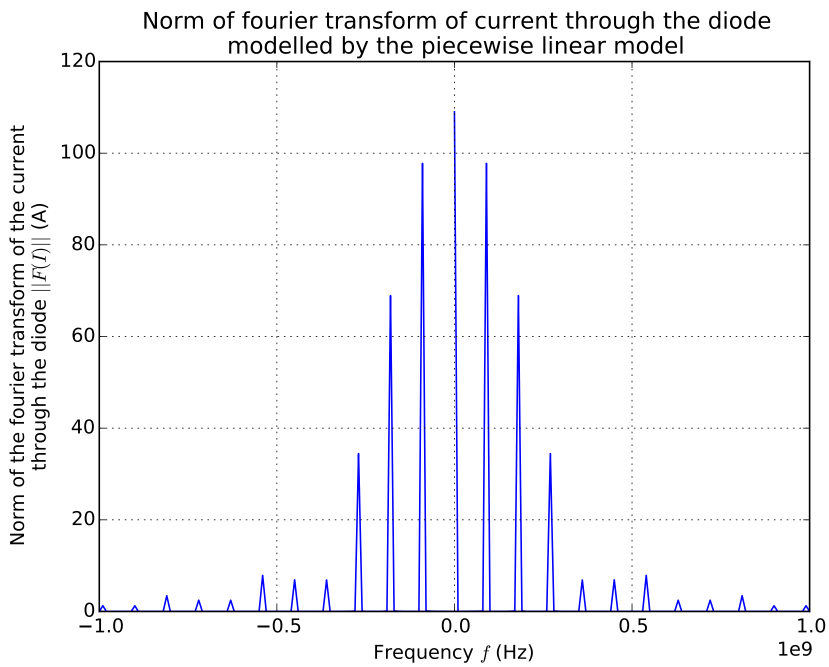


Figure 3: Fourier transform of current through the diode modelled by the piecewise linear model when radio frequency voltage with amplitude $V_{RF} = 1.0$ V and frequency $f = 100$ MHz drops across the diode.

Shockley's equation (3). Assuming that $V_{RF} \ll V_t$ [6], I obtain:

$$i_d = I_S \left( e^{\frac{V_{RF}\cos(\omega t)}{\eta V_t}} - 1 \right) \tag{5}$$

$$\approx I_s \left[ \left( \frac{V_{RF}\cos(\omega t)}{\eta V_t} \right) + \frac{1}{2!} \left( \frac{V_{RF}\cos(\omega t)}{\eta V_t} \right)^2 \right] \tag{6}$$

$$= \underbrace{\frac{I_s}{4} \left( \frac{V_{RF}}{\eta V_t} \right)^2}_{I_{DC}} + I_s \left( \frac{V_{RF}}{\eta V_t} \right) \cos(\omega_{RF} t) \tag{7}$$

where $I_{DC}$ is now the DC component of the current $i_d$ through the diode [6]. Consequently, if $V_{RF}$ is small, the DC component of the current $i_d$ through the diode is proportional to the squared voltage amplitude ${V_{RF}}^2$,

## 2.2 Diodes used

The two diodes used are HMPS2822 from Avago Technologies [10], which is based on silicon technology and used in the setup developed in [1], and CBS10S30

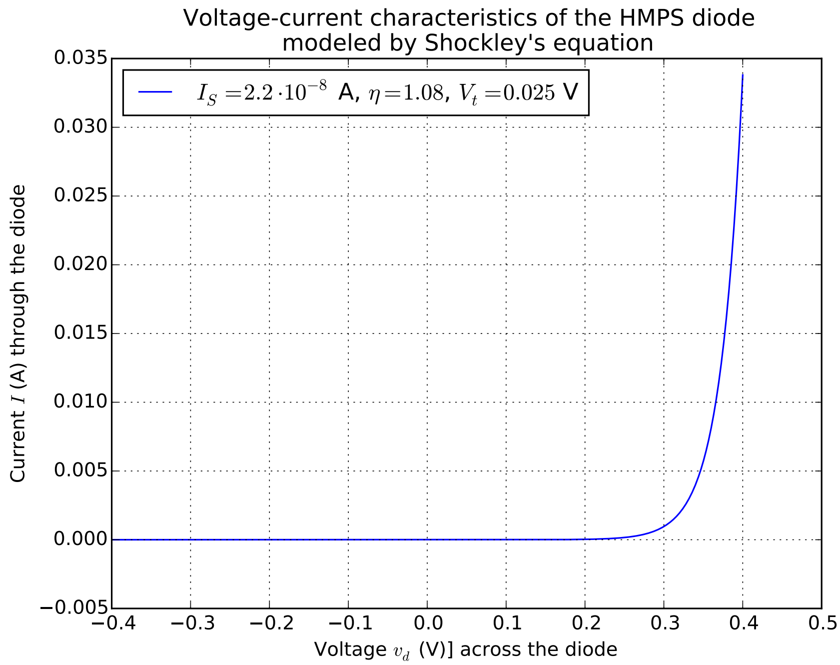


Figure 4: Voltage-current characteristics of the HMPS diode modeled by Shockley's equation with $I_S = 2.2 \cdot 10^{-8}$ A (at room temperature), $\eta = 1.08$ and $V_t = 0.025$ V (room temperature) (see [10]).

from Toshiba [12], based on silicon carbide technology known to work at cryogenic temperatures. Both diodes are Schottky barrier diodes [13], since Schottky diodes have a small reverse recovery time and thus can switch from conducting to isolating very fast [14]. Thus, they are a good choice for RF voltages.

For the measurements done, two quantities are of primary importance. The first is the reverse saturation current $I_S$ which is important due to the Shockley's equation (equation (3)). Since $I_S$ decreases strongly at cryogenic temperature, thereby decreasing the current through the diode $i_d$ a larger room temperature value of $I_S$ is a good choice. For the HMPS2822 diode, it is $I_{SO} = 2.2 \cdot 10^{-8}$ A [10, p. 3]. For the CBS10S30, the reverse saturation current is not stated in the data sheet. However, by assuming the forward voltage forward current plot in Fig. 8.1 of [12, p. 4] follows Shockley's equation, at least below a forward voltage $V_F = 0.05$ V, one can estimate the reverse saturation current (assuming $\eta = 1$). Therefore $I_{SO} \approx 2 \cdot 10^{-5}$ A for the CBS10S30 diode.

The second quantity, that this of importance, is the minimal breakdown voltage $V_{BR}$. The models discussed above both assumed that in reverse direction, the resistance of the diode is very high (even infinite in the case of the piecewise linear model). This approximation is only valid if the voltage in reverse direction is lower than the minimum breakdown voltage $V_{BR}$. If this voltage is exceeded, the diode becomes conducting again and its resistance decreases quickly. Therefore my consideration above are not valid any more and the current through the diode $i_d$ has a different dependence from the RF amplitude $V_{RF}$. For the HMPS2822 diode $V_{BR} = 15$ V [10, p. 2]and for CBS10S30 $V_{BR} = 20$ V [12, p. 1]. However, one will recognize, that the diodes are not operated in this regime for the measurement described below.

# 3 Circuit Design

In this section, I will present the circuit design for the two test circuits used and describe qualitatively how they operate.

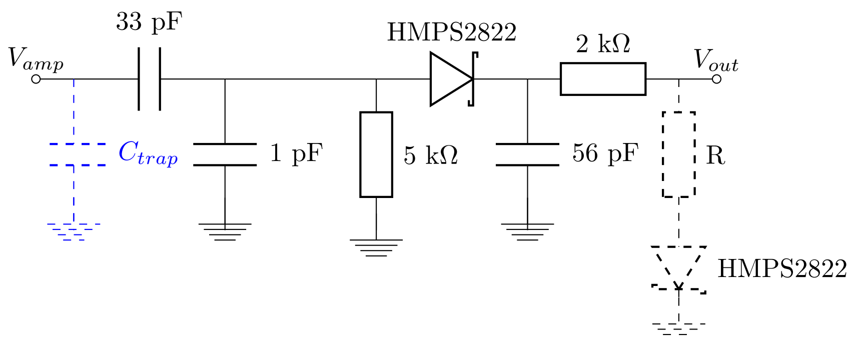


Figure 5: Schematic of the test circuit for the HMPS diode, optional components for the passive temperature compensated circuit dashed, trap dashed in blue.

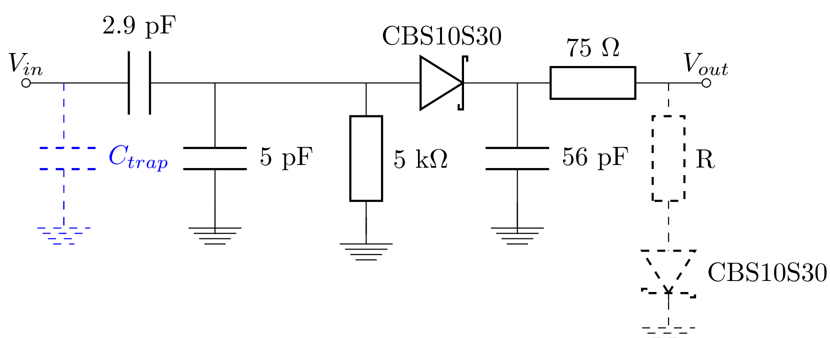


Figure 6: Schematic of the test circuit for the CBS diode, optional components for the passive temperature compensated circuit dashed, trap dashed in blue.

Fig. 5 and Fig. 6 show the two designed circuits that convert an RF voltage into a DC voltage using one diode. The principal setup of both circuits is the same as the setup used in [1]. The circuit in Fig. 5 uses the HMPS2822 diode and indeed is the circuit used in [1], but with different passive components. For ease of implementation, we did not include the second diode (and an additional resistance), dashed in Fig. 5 and in Fig. 6, for passive temperature compensation [1] in this test version, which is not necessary for finding out whether these diodes are cryo-compatible. The second circuit in Fig. 6 uses the CBS10S30 diode. Some passive components of the circuit have been changed compared to the HMPS2822 test circuit, to fit the different properties of the CBS10S30 diode (e.g. different reverse saturation current).

The circuits consist of three parts. Starting from the input $V_{amp}$, there is a voltage divider and an resistor to ground first. The voltage divider tunes the input voltage to a range in which the diode can operate. To avoid lowering the $Q$ factor of the RF resonator by lossy resistors, capacitors are used for this purpose. The 5 k$\Omega$ resistor to ground has another function: Since the input side before the diode would have only capacitors to ground without this resistor, this resistor sets the DC voltage for the diode. Without it, the diode would be DC floating. However, this resistor needs to be considered when choosing the voltage divider.

The second part of the circuits is the main part: The diode and the subsequent capacitor convert the RF voltage into a DC voltage. As described in section 2.1, both in the piecewise linear diode model and in Shokley's equation, the current through the diode $i_d$ has a DC component, that is dependent on the RF voltage amplitude, and higher frequency components (see Fig. 3 for the piecewise linear model and equation (7) for Shockley's equation). The capacitor after the diode now forms an RC-circuit with the internal resistance of the diode, which filters out higher frequency components of the current and so that the DC component is dominant in the received signal. The higher frequency components pass the capacitor and flow to ground, while the DC component of the current flows through the subsequent resistor.

The last part of the circuit is the final resistor. This resistor forms a voltage divider with the optional, dashed resistance of the passive temperature compensated circuit, which was not implemented here. This voltage divider then controls the range of measured DC voltage output $V_{out}$.

The position of the ion trap, which equivalent circuit is a capacitor $C_{trap}$, is dashed in blue in Fig. 5 and in Fig. 6. However, it could not be implemented like shown above, since the loss would be too large. One would need to adjust the voltage divider to include the trap into the test circuit.

# 4 Measurement Setup and Results

In this section, I will describe the measurement setups and report directly the corresponding measurement results. The principal setup for all measurements is shown in Fig. 7. It consists of four parts: The RF signal generator, the amplifier, the test circuit and a measurement device.

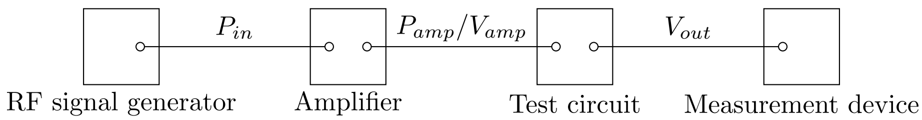


Figure 7: Schematic of the principal setup for the measurements.

The RF signal generator creates an RF voltage with power $P_{in}$ and frequency $f$. I used the RF signal generator TTi TGR1040 from Thurlby Thandar Instruments. It was able to generate pulses with frequencies $f$ between 10 MHz up to 1 GHz with a power $P_{in}$ up to 7 dBm. The peak deviation was set to 100 kHz.

Afterwards the RF voltage is amplified by an Minicircuit ZHL-1-2W-S amplifier. This is an active amplifier with a maximum input power of 10 dBm, powered by 24 V DC voltage. The amplifier was characterized and for an RF frequency of $f = 100$ MHz found to have an a linear amplification of $C = (32.90 \pm 0.04)$ dB or a voltage gain of $G = 44.1 \pm 0.2$ assuming that input and output impedance are equal. For other frequencies, the amplification varied significantly, so the amplifier was characterized for all frequencies, this time also taking into account a saturation effect for RF input powers above $P_{in} = 0$ dBm (for more details see appendix A).

After the amplifier the RF voltage with amplitude $V_{amp}$ and power $P_{amp}$ is incident on one of the two test circuit presented in the section before. Finally, the output voltage of the test circuit $V_{out}$ will be measured by different measurement devices, corresponding to the specific measurement done. Since the measurements were done in part at cryogenic temperatures, I first explain how this was done.

## 4.1 Measurements in liquid helium

The measurements in liquid helium were done using a dewar of liquid helium, a long plastic pipe and long cables. The designed circuit was connected to the long cables and then put deeply into the pipe. After that, the cables running through the pipe were connected to the respective devices and the devices were switched on. Finally, the pipe was slowly dunked into the liquid helium dewar (with the circuit at the lower end) in accordance with safety rules.

When dunking the pipe into the dewar, helium absorbs heat from the circuit and the pipe and gets boiled. After waiting until the system gets steady, one can assume that the circuit is thermalized with liquid helium and is cooled down to liquid helium temperature, i.e. 4.2 K. In addition to these measurements, I also tested the cold start of the circuit in liquid helium.

## 4.2 Amplified input power $P_{amp}$ vs. Output voltage $V_{out}$

### 4.2.1 Motivation

To verify whether the output voltage of the test circuit samples the RF amplitude with sufficient precision (up to 10 mV at an RF amplitude of 100 V, see Introduction) at cryogenic temperatures, it is necessary to measure the dependence between the amplified input power $P_{amp}$, which can be related to the RF amplitude by the impedance used, and the DC output voltage $V_{out}$. The dependency determines how precisely the DC output voltage has to be measured in order to achieve the intended sampling precision.

### 4.2.2 Setup

To measure DC output voltages $V_{out}$ for different amplified RF input powers $P_{amp}$, a Uni-T UT39C multimeter was used as measurement devices. The measurement was done for both test circuits (HMPS2822 and CBS10S30). The measurement was done at liquid-helium temperature for both test circuits at a frequency of $f = 100$ MHz and for comparison for different frequencies at room temperature.

### 4.2.3 Results

#### Room Temperature

**HMPS Diode** The measured DC output voltage $V_{out}$ for different amplified RF input powers $P_{amp}$ for the HMPS diode circuit at room temperature are shown in Fig. 8. The measurement was done for different frequencies at $f = 40$ MHz, $f = 60$ MHZ, $f = 80$ MHz and $f = 100$ MHz.

I observe, that the output varies significantly for different frequencies. Furthermore, I notice an exponential dependence between amplified input power $P_{amp}$ and the output voltage $V_{out}$.

**CBS diode** Similar to Fig. 8 for the HMPS diode, Fig. 9 shows the measured DC output voltage $V_{out}$ for different amplified RF input powers $P_{amp}$ for the CBS diode circuit. Again, the measurements were done at room temperature and again for different frequencies at $f = 40$ MHz, $f = 60$ MHZ, $f = 80$ MHz and $f = 100$ MHz.

I notice, that again the output voltage clearly is frequency dependent and this time the output voltages $V_{out}$ are much lower compared to HMPS diode circuit. The dependence between input power $P_{amp}$ and output voltage $V_{out}$ is again approximately exponential with the exception of a visible saturation above $P_{amp} = 30$ dBm for $f = 40$ MHz.

#### Liquid-Helium Temperature Test

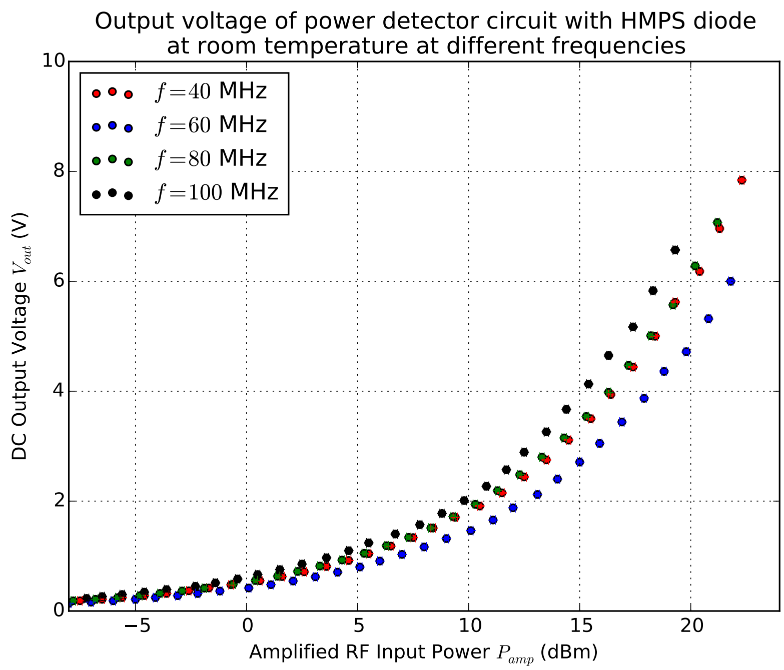


Figure 8: DC output voltage $V_{out}$ for different amplified input powers $P_{amp}$ and for different frequencies $f$ for the HMPS diode circuit at room temperature.

**HMPS Diode** Fig. 10 shows again the measured DC output voltage $V_{out}$ for different amplified RF input powers $P_{amp}$ at a frequency $f = 100$ MHz for the HMPS diode circuit, but this time at room temperature and in liquid helium. One observes that in liquid helium, there is almost no output voltage $V_{out}$ measured below -10 dBm input power. Above -10 dBm input power, the measured output voltage in liquid helium increases, but it is still smaller than the DC output voltage measured at room temperature at -20 dBm input power. Finally, there is a huge jump in the output voltage for liquid helium: At $P_{amp} =$ 29 dBm, the output voltage is $V_{out} = (1.632 \pm 0.001)$ V, while it is $V_{out} =$ $(9.54 \pm 0.01)$ V at $P_{amp} = 30$ dBm. A cold start did not influence the results significantly.

**CBS Diode** As above for the HMPS diode, in Fig. 11 the measured DC output voltage $V_{out}$ for different amplified RF input powers $P_{amp}$ is illustrated at room temperature and in liquid helium for the CBS diode. Again, the measurements were done at a frequency of $f = 100$ MHz.

One notices that the dependency between the two quantities is complicated. However, one may observe that the curves for room temperature and for liquid helium have a similar shape, although the output voltage $V_{out}$ in liquid helium

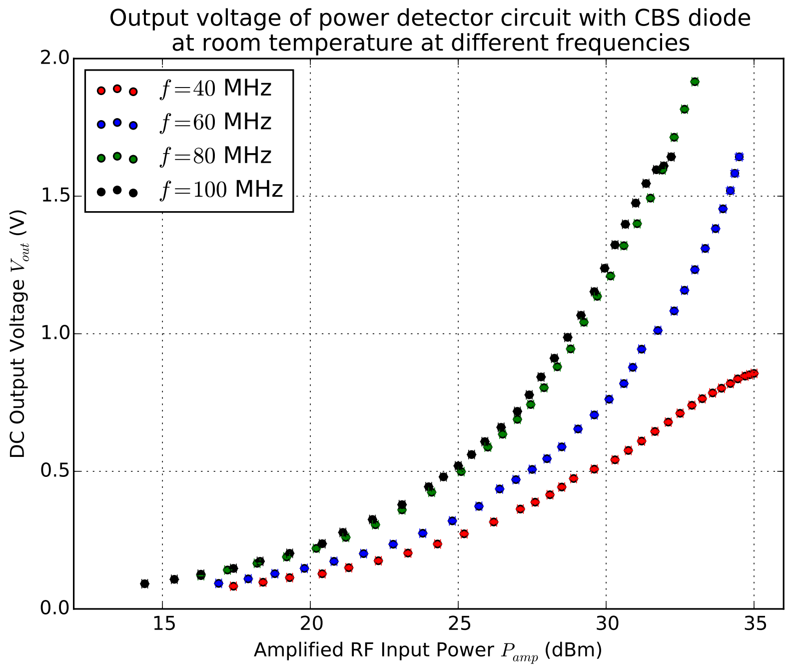


Figure 9: DC output voltage $V_{out}$ for different amplified input powers $P_{amp}$ and for different frequencies $f$ for the CBS diode circuit at room temperature.

is larger than at room temperature. Also, the output voltage seems to vary more in liquid helium for different input powers $P_{amp}$. Again a cold start did not change the results.

## 4.3 Stability measurements

### 4.3.1 Motivation

Stability measurements are central to decide whether the test circuits are able to sample the RF voltage accurately over long time periods and thus whether they can be used as a part of an feedback control setup that stabilizes the RF voltage. For an unstable rectifying circuit, one cannot decide whether a drift in its output voltage comes from the drift of input RF voltage, and thus needs adjustment, or from the rectifying circuit itself. In the last case, any adjustment would indeed destabilize the RF voltage. Therefore, the amplitude of any fluctuation or drift in the output voltage $V_{out}$ effectively limits the sampling precision.

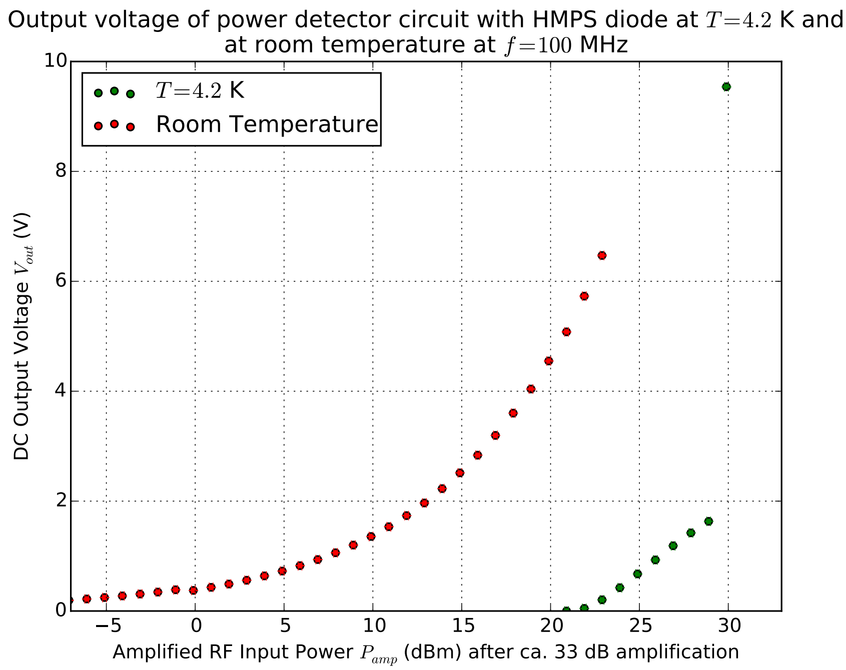


Figure 10: DC output voltage $V_{out}$ for different amplified input powers $P_{amp}$ for the HMPS diode circuit at room temperature and in liquid helium.

### 4.3.2 Setup

To measure the stability of the output voltage $V_{out}$ at fixed amplified RF input power $P_{amp}$, an oscilloscope and a spectrum analyzer were used as measurement devices. The spectrum analyzer was used to watch for fast variations at the order 1 to 100 kHz. The oscilloscope and a filter, which was used to suppress remaining RF voltage components, in contrary was applied to look for variations or drifts on a timescale of $\tau = 1000$ s.

The oscilloscope used was a Tektronix DPO2014B with a cut-off frequency of 100 MHz. Therefore, an additional filter, consisting of an RC circuit with $R = 1$ k$\Omega$ and $C = 182$ pF, was used. The spectrum analyzer was a FieldFox N9912A. The measurement with the oscilloscope was only performed in liquid helium, while the measurements with the spectrum analyzer were done both at room temperature and in liquid helium. Also, the measurement was done only for the CBS10S30 diode test circuit.

### 4.3.3 Results

**Spectrum Analyzer** The result of the spectrum analyzer measurement is shown in Fig. 12. The plot shows the Fourier transform of the power $P_{out}$

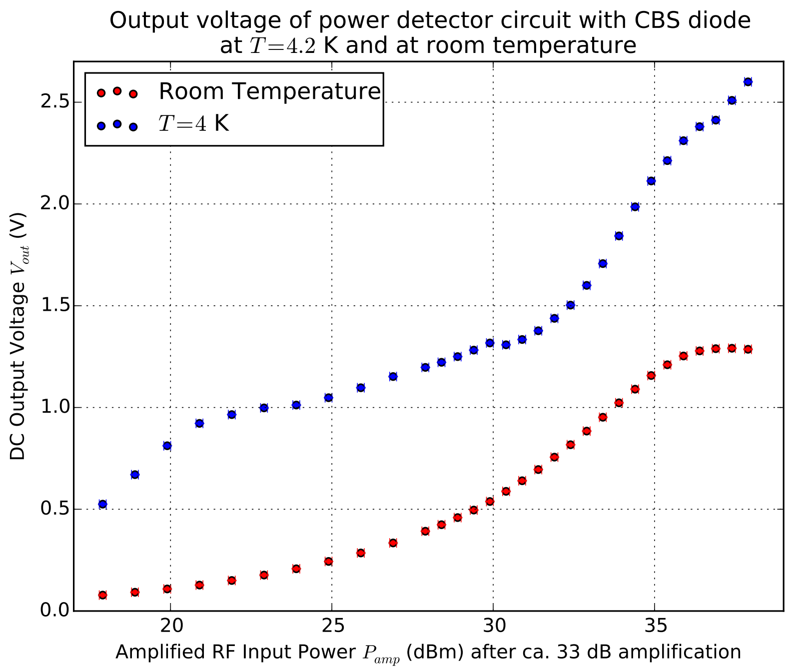


Figure 11: DC output voltage $V_{out}$ for different amplified input powers $P_{amp}$ for the CBS diode circuit at room temperature and in liquid helium.

at the output of the circuit for frequencies from 100 Hz to 100 kHz for room temperature and in liquid helium. One observes that the output for both temperatures is around -80 dBm for all frequencies, with a slow increase to -70 dBm towards 0 Hz. However, this measurement result cannot be distinguished from the measurement without any input at the spectrum analyzer. Thus, I conclude that there are no visible fluctuations in the frequency range from 100 Hz to 100 kHz.

**Oscilloscope** Fig. 13 shows the total output voltage $V_{out,Tot}$ in dependence of time $t$ at fixed input power $P_{in} = -10$ dBm. 125,000 data points were taken in a time period of $t = 1000$ s.

One recognizes, that all values are inside a large bulk with an amplitude of around 0.001 V, that varies slowly around 0.970 V. These variations happen on a timescale of 100 s, and do have an amplitude of circa 1 mV. One also notices, that these variations occur quite randomly.

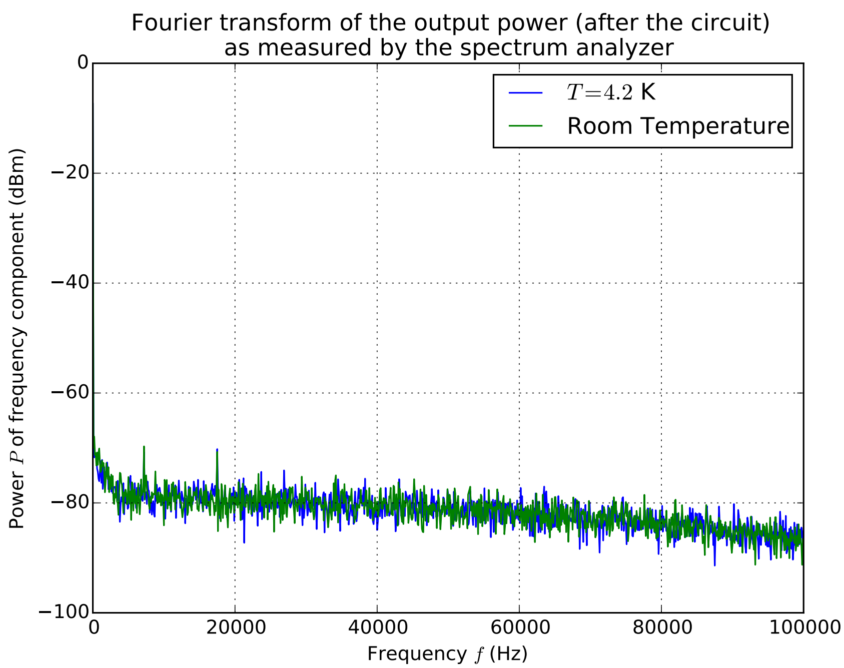


Figure 12: Fourier transform of the output power (after the circuit) as measured by the spectrum analyzer at fixed input power $P_{amp} = 23$ dBm for room temperature and in liquid helium.

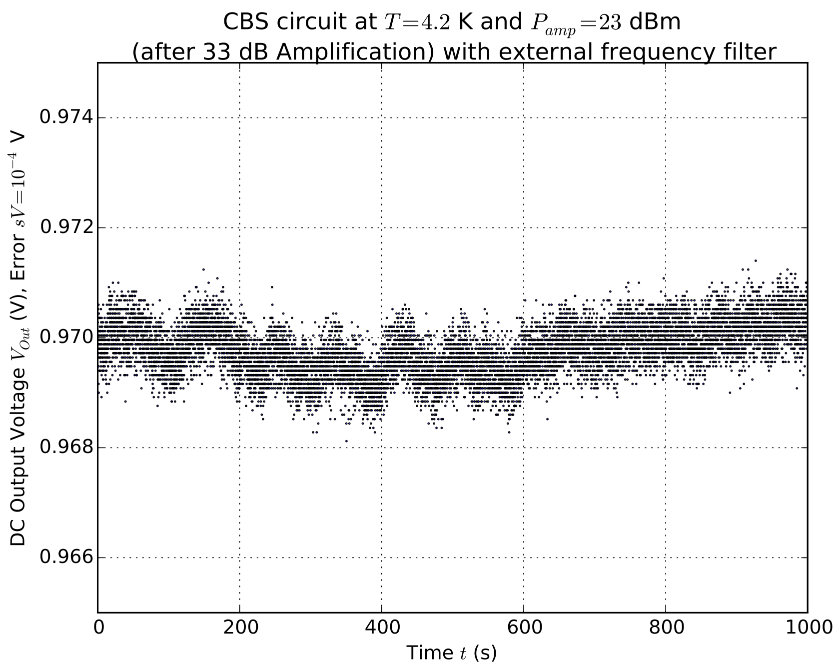


Figure 13: Time dependence of total output voltage $V_{out,Tot}$ for the CBS diode circuit in liquid helium at fixed input power $P_{amp} = 23$ dBm.

# 5 Analysis and Discussion

In this section, I will analyze the results described above with the aim of verifying whether the test circuit can be used to sample the RF voltage precisely enough at cryogenic temperature or not.

## 5.1 Amplified voltage on the circuit

It will be useful to plot the output voltage $V_{out}$ against the RF voltage amplitude $V_{amp}$ incident on the circuit for two reasons. First, and more importantly, the aim of the thesis is to verify if the test circuit sample the RF voltage amplitude precisely enough. Therefore, it is convenient to plot the DC output voltage $V_{out}$ against the amplified RF voltage amplitude $V_{amp}$. Secondly, one will be able to decide, in what range one can describe the diode by the piecewise-linear model or by Shockley's equation.

In general, one has to consider two effects when calculating the amplified voltage incident on the circuit $V_{amp}$ since the input impedance of the designed circuit is not 50 $\Omega$. First, a part of the power $P_{amp}$ is reflected on the circuit and thus not propagating into the circuit. Furthermore, the incident voltage depends on the input impedance, for a certain amount of input power.

To calculate the input impedance exactly is not possible, since the diode is a non-linear element and does not have aa well-defined impedance. Thus, I will make the assumption that the diode has an infinite impedance. This is motivated by the fact that the diode is not conducting half of the time (at least), see Fig. 2. So the effective, time-averaged impedance of the diode will be very large. Besides, the fact that the obtained $V_{amp}$ are reasonable with respect to the measured DC output voltages, as can be observed in Fig. 16, supports the assumption.

If I assume the diode has an infinite impedance, I can easily calculate the input impedance $Z$ of the circuit and the ratio of power reflected by the circuit and the total input power $R$. I get:

$$Z = \frac{1}{\imath\omega C_1} + \frac{1}{\imath\omega C_2 + \frac{1}{R_1}}, \tag{8}$$

where $C_1$ is the capacitor directly after the input of the circuit, $C_2$ the subsequent capacitor to ground, $R_1$ the resistor in parallel to $C_2$ and $\omega$ the angular frequency of the RF voltage. Correspondingly the ratio of power reflected by the circuit is:

$$R = \left| \frac{Z - Z_0}{Z + Z_0} \right|^2, \tag{9}$$

where $Z_0$ is the impedance of the wire, i.e. 50 $\Omega$. I find that for both diodes more than 95 % of the power is reflected.

Finally, I can calculate the amplified voltage on the circuit, assuming the diode has infinite impedance. It is:

$$V_{amp} = \sqrt{R \cdot 10^{\frac{P_{amp}[\text{dBm}]}{10 \text{ dBm}}} \cdot \frac{Z \cdot \text{W}}{1000}} \cdot \sqrt{2} \tag{10}$$

Consequently, one may observe the main dependencies between DC output voltage $V_{out}$ and RF input voltage $V_{amp}$.

In this formula, I also assume an infinite wire, such that there is no standing wave in the wire that reduces the power transmitted into the circuit. In section 5.2.3, however, I conclude that there is indeed a standing wave in the wire. Since the length of the wire and the standing wave in it was not further investigated, I cannot include this effect into the calculation. Therefore, the calculated values could be shifted by at least 2-3 dBm as explained in section 5.2.3.

## 5.2 CBS Diode

### 5.2.1 Amplified voltage vs. output voltage at liquid-helium temperature and at room temperature.

Fig. 14 shows the dependency between amplified input voltage $V_{amp}$ and DC output voltage $V_{out}$ at $f = 100$ MHz both at room temperature and at liquid-helium temperature for the CBS10S30 test circuit. One recognizes, that like in Fig. 8, the output voltage at room temperature is much smaller compared to the HMPS2822 test circuit. This has a simple reason: One recognizes in Fig. 6 the test circuit for the CBS10S30 diode has a voltage divider of around 1:3, while there is an almost 1:1 voltage divider in the HMPS2822 test circuit. Furthermore, the saturation current and the value of the final resistor are different, so one cannot compare the outputs directly.

The room temperature curve in Fig. 14 shows a quadratic dependence below $V_{amp} = 5$ V, a linear dependence between $V_{amp} = 10$ V and $V_{amp} = 15$ V and then slowly saturates. The quadratic behavior at RF voltages is consistent with Shockley's equation, while the linear slope is consistent with the piecewise-linear diode model. For the saturation, there are several possible explanation: Most likely, it is due to a saturation of the amplifier, which was not taken into account here (see appendix A). Another explanation is that, since the reverse breakdown voltage of the CBS10S30 diode is 20 V, at $V_{amp} = 25$ V, I came closer to the breakdown limit, but taking into account the 1:3 voltage divider, not significantly close. However, there could be an effect due to this.

The slope of the linear part of the curve is roughly 0.08. Assuming that one can measure the DC output voltage with a precision of 1 mV, one obtains a precision of around $8 \cdot 10^{-4}$ at $V_{amp} = 15$ V (corresponding to $P_{amp} \approx 33.5$ dBm). One will recognize below, that this is worse than the HMPS2822 test circuit.

The liquid-helium temperature curve in Fig. 14 has a more diverse shape than the room temperature curve. One cannot divide the curve easily into three regions. However, one recognizes, that there is a relationship with the room

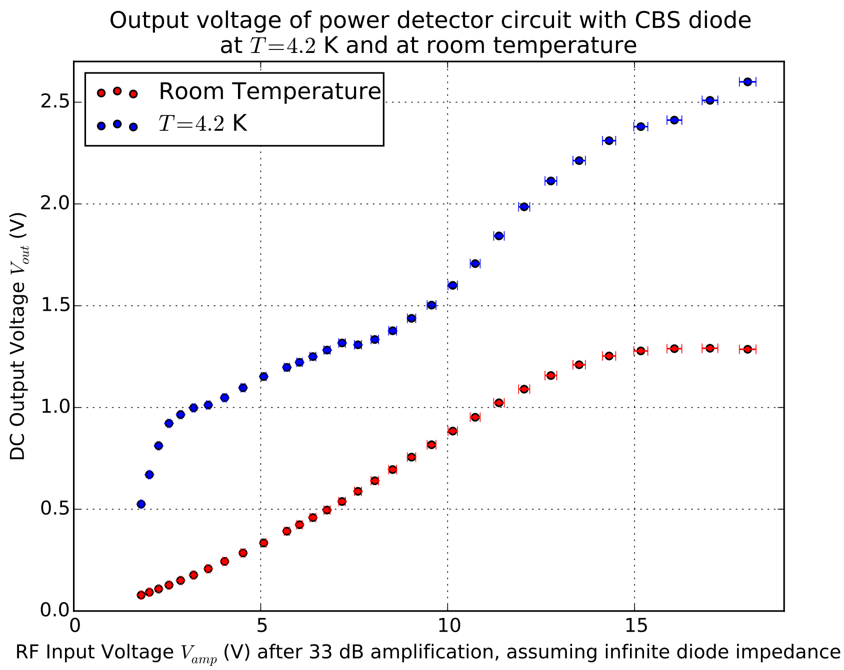


Figure 14: DC output voltage $V_{out}$ for different amplified input voltages $V_{amp}$ assuming 50 $\Omega$ impedance for the CBS diode circuit at room temperature and in liquid helium.

temperature curve. At liquid-helium temperature, some additional fluctuations and drifts seem to have added to the curve.

The reason for this variations could be thermal fluctuations and heating. Since a current flows through the test circuit, this current could heat up the liquid helium around the circuit slightly and thus change its properties. Since the measurement was started at low input power and then successively increasing it, I could have slowly heated up the liquid helium around the circuit.

Between $V_{amp} = 13$ V and $V_{amp} = 18V$, the 4 K curve is roughly linear with a slope of around 0.1. As above, assuming I can measure the DC output voltage up to a precision of 1 mV, this results in a precision of around $5 \cdot 10^{-4}$ at $V_{amp} = 17$ V (corresponding to $P_{amp} = 34.5$ dBm). This is one order away from the precision required for the experiment (around $1 \cdot 10^{-5}$ at $V_{RF} = 100$ V).

To conclude, the CBS10S30 test diode circuit is promising for both room temperature and liquid-helium temperature. If the CBS10S30 test diode circuit is stable enough at liquid-helium temperature (maximal variations of the order 1 mV in the DC output at constant RF input), this circuit could be useful for the experiment.

#### 5.2.2 Stability

For the spectrometer measurements (Fig. 12) I observed that there are no significant fluctuations in the range from 100 Hz to 100 kHz. Therefore, one can conclude, that for short timescales, the output voltage is indeed stable, only an RF voltage component remains, that can be filtered out easily.

For the oscilloscope, one observed in Fig. 13, a large, slowly varying bulk of measurement points. The bulk comes from the RF voltage component. Although a filter was used, the RF amplitude was not completely suppressed due to noise pick-up of the oscilloscope. Therefore, the oscilloscope, which was able to resolve the RF voltage, randomly took a measurement at some point in the RF voltage curve, resulting in this bulk. I could confirm that the bulk is the RF component with the oscilloscope by measuring the frequency of the fastly oscillating curve which produces the bulk.

Of greater importance, are the drifts of this bulk. Those variations have an amplitude of 1 mV and appear quite randomly. An explanation for these variations could be thermal variations both around the circuit in liquid-helium and around cables and devices at room temperature or at intermediate temperatures in the pipe. Since thermal variations in liquid helium are usually small due to the properties in liquid helium and this time the applied power is kept constant, so there is no significant heating, it is likely that those variations come from cables and devices at room temperature or from cables in the pipe.

In conclusion, variations are of the order of 1 mV, so the precision of around $5 \cdot 10^{-4}$ at $V_{amp} = 17$ V is correct. This is one order larger than desired. However, if one manage to stabilize the circuit further, for example by stabilizing temperature, one can achieve better precision. By using a highly stable voltage reference (as done for the HMPS2822 in [1]), one can measure DC voltages on the $\mu$V range and thus achieve the desired precision. Therefore the CBS10S30 diode test circuit is a good candidate for further testing.

#### 5.2.3 Frequency dependence

In Fig. 9, where DC output voltage $V_{out}$ is shown in dependence of amplified power $P_{amp}$ at different frequencies, I observed above an approximately exponential behavior for all frequency (with the exception of $f = 40$ MHz). This corresponds to a linear dependence between amplified voltage $V_{amp}$ and output voltage $V_{out}$ as predicted by the piecewise-linear model. Here the saturation of the amplifier was taken into account (see appendix A) and as a result, except for a frequency of $f = 40$ MHz, I observed no saturation. Hence, the saturation at $f = 100$ MHz described in Fig. 14 (where the saturation of the amplifier was not taken into account) for the room temperature curve is indeed due to the saturation of the amplifier. For $f = 40$ MHz, I found a deviation from the exponential behavior, which corresponds to a saturation. However, this effect could be due to a broken cable connection in the measurement for $f = 40$ MHz.

Above I also mentioned that the results vary significantly for the different frequencies. One reason for this is the unmatched impedance on the test circuit.

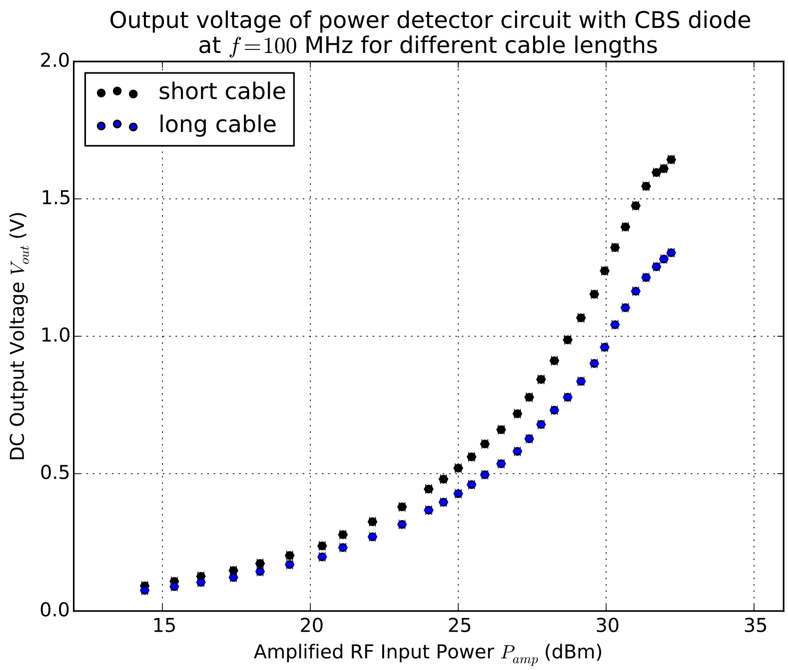


Figure 15: DC output voltage $V_{out}$ for different amplified input powers $P_{amp}$ for the CBS diode circuit at room temperature at a frequency $f = 100$ MHz for a short and a long cable.

Consequently, the fraction of the amplified power $P_{amp}$ transmitted into the test circuit is dependent on the ratio $\frac{l}{\lambda}$ where $l$ is the length of the cable between the amplifier and the test circuit and $\lambda$ the wavelength of the RF frequency used. Therefore, the fraction of the amplified power $P_{amp}$ transmitted into the test circuit is different for different frequencies, which then results into the different DC output voltages $V_{out}$ as observed above.

Fig. 15 demonstrates the effect of the unmatched impedance on the DC output voltage $V_{out}$. Here, the DC output voltage $V_{out}$ was measured at a frequency of $f = 100$ MHz at room temperature for a short cable, connecting the amplifier and the test circuit, and a cable, that was about 0.5 m longer. Other properties were not changed. I observe that the curve for the short cable, compared to the curve of the long cable, is shifted to the left by 2 to 4 dBm. Since the fraction of the amplified power $P_{amp}$ transmitted into the test circuit depends on $\frac{l}{\lambda}$, the variation of the frequency can result in a similar shift than observed here.

To conclude, the unmatched impedance on the test circuit results in different DC output voltages $V_{out}$ for different frequencies as observed in Fig. 9. From Fig. 15, I conclude that these variations are at least in the order of 2 to 4 dBm.

Therefore, it is possible that the frequency dependency observed in Fig. 9 arises only due to the unmatched impedance. However, from the measurements done here, it is not possible to decide whether the unmatched impedance is the only effect contributing to the frequency dependence. In particular, I cannot decide whether the test circuit itself produces a frequency dependent or a frequency independent DC output voltage $V_{out}$.

### 5.3 HMPS Diode

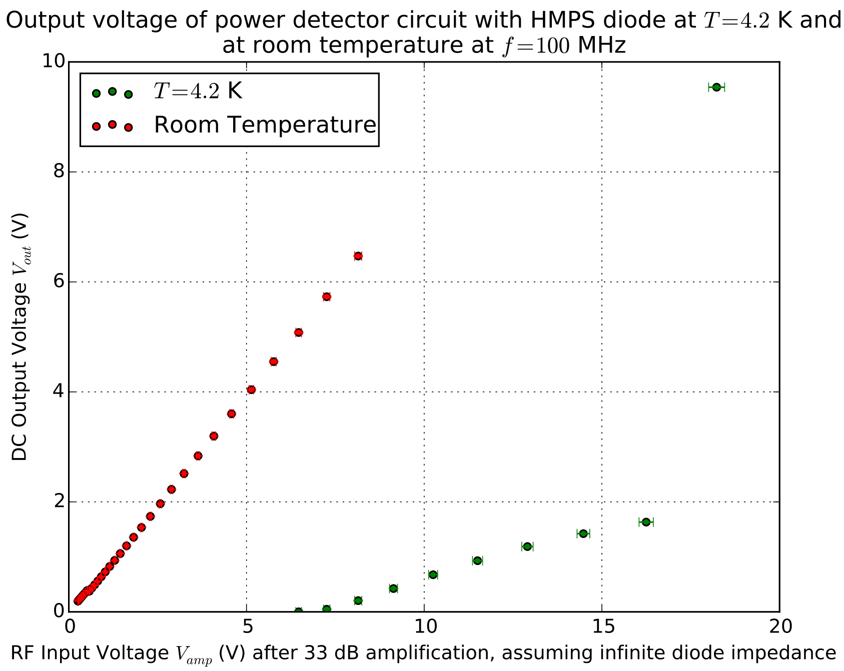


Figure 16: DC output voltage $V_{out}$ for different amplified input voltages $V_{amp}$ assuming 50 Ω impedance for the HMPS diode circuit at room temperature and in liquid helium.

As Fig. 14 for the CBS10S30 test circuit, Fig. 16 shows the output voltage $V_{out}$ for different amplified voltages $V_{amp}$ at a frequency $f = 100$ MHz for the HMPS2822 test diode circuit at room temperature and in liquid helium. I observe, that for room temperature there is a linear relationship between output voltage $V_{out}$ and amplified voltages $V_{amp}$, at least above $V_{amp} = 1$ V. This behavior is consistent with the exponential dependence between output voltage $V_{out}$ and input power $P_{amp}$ in Fig. 8.

Therefore, the piecewise-linear model, which produces a linear relationship between RF amplitude $V_{RF}$ and the DC component of the current through the diode $I_{Out,DC}$ (see equation (2)) and consequently (considering an Ohmic resistance) the output voltage $V_{out}$, is valid in this range at room temperature. Below $V_{amp} = 1$ V at room temperature, the dependence is not linear, a quadratic dependence as predicted by Shockley's equation (7) is possible.

The frequency dependency in Fig. 8 is similar to the observed dependency in Fig. 9 for the CBS10S30 diode. As a consequence, I can conclude that the unmatched impedance on the test circuit contributes to the frequency dependency of the DC output voltage $V_{out}$ as observed for the CBS10S30 diode. However, from the measurements done, I am again not able to decide, whether the circuit itself contributes to the frequency dependency or not.

The slope of the linear part of the plot in Fig. 16 at room temperature is roughly 1.4. Therefore, if I am able to measure the DC output voltage up to a precision of 1 mV, I can measure the RF voltage amplitude with a precision of 0.7 mV. Assuming that is true at an amplified RF input voltage of 4 V, this means a precision of around $2 \cdot 10^{-4}$. However, this is only true, if the variations in the DC output voltage at constant RF input voltage are significantly smaller than 1 mV.

For the liquid-helium measurement, no such linear relationship is observable. As observed before, the DC output voltage is much smaller than at room temperature at the same RF input voltage. An explanation for this is the low saturation current of the HMPS2822 diode at room temperature. At cryogenic temperature it further decreases, thus effectively decreasing the current through the diode. Therefore, the diode has a higher resistance and the output voltage becomes smaller.

Furthermore, the jump in the output voltage observed before in Fig. 16, is also visible here. Due to the large slope, this is a potentially interesting region. However, I think, this jump is due to some heating effect. The measurement was done starting at low input powers and then successively increasing the input power. So, a slow heating of the circuit due to the relatively high input power, could have happened, thus leading to a higher saturation current (and lower resistance) and therefore a higher output voltage. Therefore the slope would be useless. However, further investigation could be useful.

To conclude, the HMPS2822 diode test circuit is able to sample the RF voltage amplitude at room temperature with a precision of $2 \cdot 10^{-4}$ at 4 V amplified RF voltage, while at liquid-helium temperature further investigation is needed. If the jump corresponds to a heating effect, than the low slope and the sudden jump make it very difficult to use this test circuit. If the jump is not a temperature dependent effect, than the diode could be a possible candidate. Therefore, the diode was for sure a good choice in Maryland [1], since they are operating at room temperature, but for our setup that operates at liquid-helium temperature additional measurements are necessary.

# 6 Conclusion

Finally, I showed that the CBS10S30 diode is cryo-compatible, while the HMPS2822 diode is not. Furthermore, I concluded that the CBS10S30 diode test circuit samples the RF voltage faithfully and with a precision of $5 \cdot 10^{-4}$ at $V_{amp} = 17$ V, which is one order away from the desired precision of $1 \cdot 10^{-5}$ at $V_{amp} = 100$ V. By using a highly stable voltage reference and stabilizing temperature, the precision can be increased and this qualifies the circuit for further testing.

A next step, beside temperature stabilization and introducing a highly stable voltage reference, is to set up a feedback loop with the test circuit, inject noise into loop and measure the noise reduction due to the feedback loop both at cryogenic temperature and at room temperature (for comparison). Furthermore, one needs to investigate if the temperature compensated circuit proposed in [1] is working at cryogenic temperatures and if this circuit further increases the precision significantly. If all measurements show respective results, one can finally think on how to set the voltage divider in order to achieve large enough precision, avoid overcharging the ion trap and not to distract too much power from the ion trap.

In addition to this, one could also investigate other diodes and test circuits and the jump observed for the HMPS2822 diode with the aim of increasing the sampling precision further. However, the CBS10S30 diode test circuit, according to the measurements done in this thesis, is a promising candidate.

# Appendices

## A Amplification

To measure the amplified power $P_{amp}$, the RF source was connected directly to the amplifier. The output of the amplifier was then connected to the spectrum analyzer. The spectrum analyzer then measured $P_{amp}$ for different input powers $P_{in}$. This is easier than measuring the RF voltage amplitude with the oscilloscope, since one has a large amount of power reflected to the unmatched impedance in this case.

To calculate the amplified power $P_{amp}$ for the plots two methods were used: For the measurements comparing room temperature and liquid helium temperature at $f = 100$ MHz (i.e. in Fig. 10, Fig. 11, Fig. 16 and Fig. 14) a linear fitting was applied to $P_{amp}$ vs. $P_{in}$ plot. As described in subsection A.1, this resulted in a gain of $C = (32.90 \pm 0.04)$ dB, which was then simply added to the input power $P_{in}$ to obtain $P_{amp}$. Since a linear fitting was used, any possible saturation of the amplifier was not accounted for.

For the frequency dependent plots, a different method was used: The amplified power $P_{amp}$ was measured for different frequencies at different input powers $P_{in}$. The amplified power $P_{amp}$ corresponding to the applied input power was then used in the plots (i.e. in Fig. 8, Fig. 9 and Fig. 15). This is described in subsection A.2. Here, the saturation of the amplifier is taken into account, since I use the measured values of $P_{amp}$ directly.

## A.1 Linear fitting of the amplification for $f = 100$ MHz

In Fig. 17, one can see the power coming out of the amplifier $P_{amp}$ in dependence of the power at the input of the amplifier $P_{in}$ for a frequency of $f = 100$ MHz. One recognizes, that the measured data is in good accordance with the linear fitting curve $y = x + C$ where $C = (32.90 \pm 0.04)$ dB.

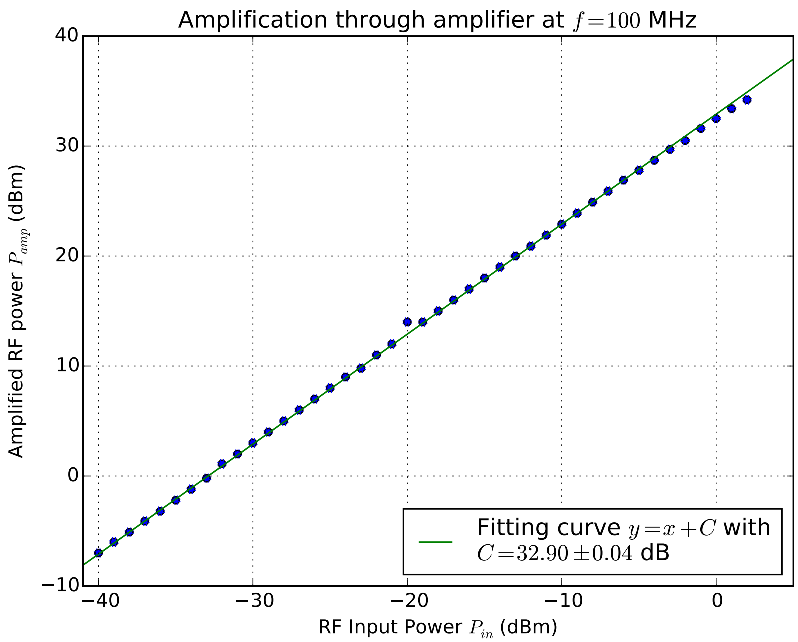


Figure 17: Amplified power $P_{amp}$ against unamplified power $P_{in}$ for a frequnecy of $f = 100$ MHz.

Since the amplification agrees quite accurately with the fitting curve, there is a linear amplification of $C = (32.90 \pm 0.04)$ dB. If one converts this amplification into gain factor for voltages, one considers the conversion formula for power in dBm $P$[dBm] to the corresponding voltage $V$ in V assuming input and output impedance of the amplifier to be equal:

$$V = \sqrt{P[\mathrm{W}]R} = \sqrt{\frac{1\mathrm{W}}{1000} \cdot 10^{\frac{P[\mathrm{dBm}]}{10\ \mathrm{dBm}}} \cdot R} \tag{11}$$

where $P$[W] is the power in W. So if one assumes the amplified power $P_{amp} =$

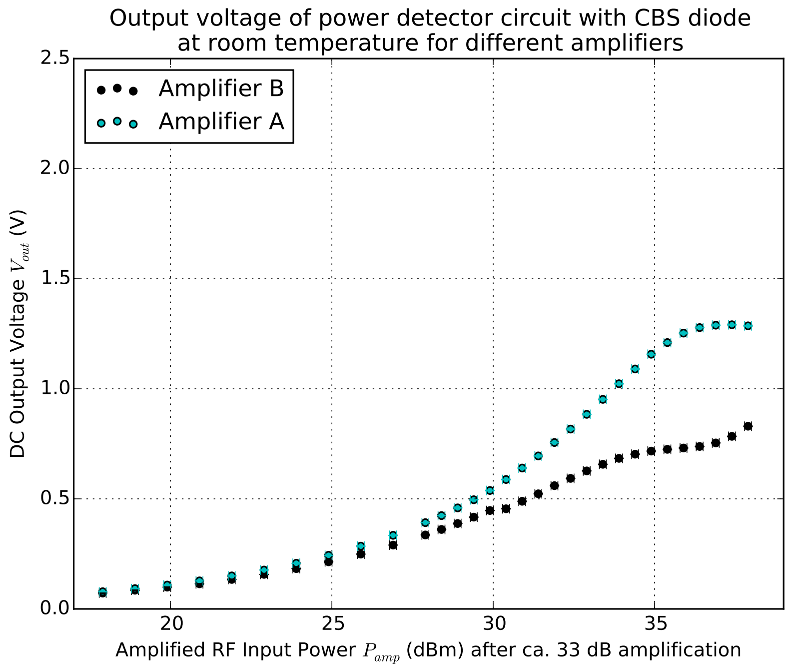


Figure 18: DC output voltage at $f$ = 100 MHz at room temperature for the amplifier used for the measurements at different temperatures, labelled "Amplifier A", and for the amplifier used to determine the amplifier gain, labelled "Amplifier B".

$P_{in} + C$, than for the amplified voltage $V_{amp}$, one obtains:

$$V_{amp} = \sqrt{\frac{1\mathrm{W}}{1000} \cdot 10^{\frac{P[\mathrm{dBm}]+C}{10\ \mathrm{dBm}}} \cdot R} \tag{12}$$

$$= \sqrt{\frac{1\mathrm{W}}{1000} \cdot 10^{\frac{P[\mathrm{dBm}]}{10\ \mathrm{dBm}}} \cdot 10^{\frac{C}{10\ \mathrm{dBm}}} \cdot R} \tag{13}$$

$$= \sqrt{\frac{1\mathrm{W}}{1000} \cdot 10^{\frac{P[\mathrm{dBm}]}{10\ \mathrm{dBm}}} \cdot R} \cdot \sqrt{10^{\frac{C}{10\ \mathrm{dBm}}}} \tag{14}$$

$$= V_{unamp}\sqrt{10^{\frac{C}{10\ \mathrm{dBm}}}} \tag{15}$$

where $V_{unamp}$ is the unamplified voltage, and $R$ the input and output impedance. So one obtains a linear amplification with a gain factor $G$ of $G = \sqrt{10^{\frac{C}{10\mathrm{dBm}}}} = 44.1 \pm 0.2$.

For this measurement, the amplifier used, was different from the one used for the measurements on the DC output voltage at different temperatures. However, both amplifiers were of the same type (Minicircuit ZHL-1-2W-S), only a different exemplar was used, so one may still assume linear amplification. Only the constant $C$ or the gain factor $G$ may have changed. Fig. 18 shows the DC output voltage at $f = 100$ MHz at room temperature for the amplifier used for the other measurements, labeled "Amplifier A", and for the amplifier used to determine the gain, labeled "Amplifier B". It shows that the DC output voltage $V_{out}$ of the different amplifiers is different. So, the constant $C$ may indeed have changed. However, the unmatched impedance on the circuit could also have contributed to this difference, since the cables used for the measurements of the different amplifiers were of different length.

## A.2 Direct plotting of the amplifiied voltage

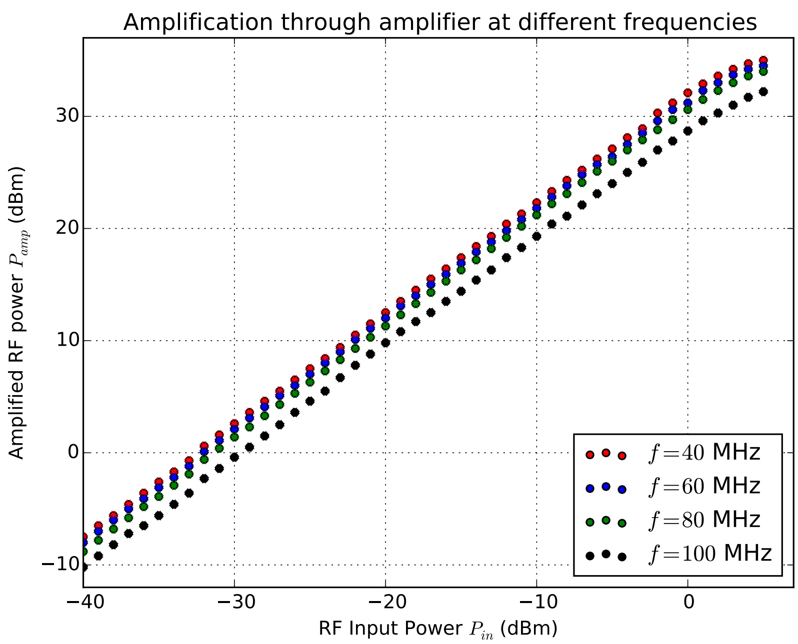


Figure 19: Amplified power $P_{amp}$ against unamplified power $P_{in}$ for different frequnecies.

Fig. 19 shows the amplified power $P_{amp}$ for different input powers $P_{in}$ at different frequencies. The amplifier was again a Minicircuit ZHL-1-2W-S, but a different exemplar than the ones mentioned in A.1. However, the same amplifier was used for the frequency dependent measurements (i.e. Fig. 8, Fig. 9 and Fig. 15), for which this measurement was used. So the plots are consistent.

As described above, in the frequency dependent measurements, the DC output voltage was measured for a particular input power $P_{in}$. Then, the corresponding value for the amplified power $P_{amp}$ (shown in Fig. 19) was plotted against the DC output voltage $V_{out}$. If the DC output voltage was measured for some intermediate value of $P_{in}$, for which $P_{amp}$ has not been measured, the average of the two nearest measurement points was used.

# B PCB design of the test circuits

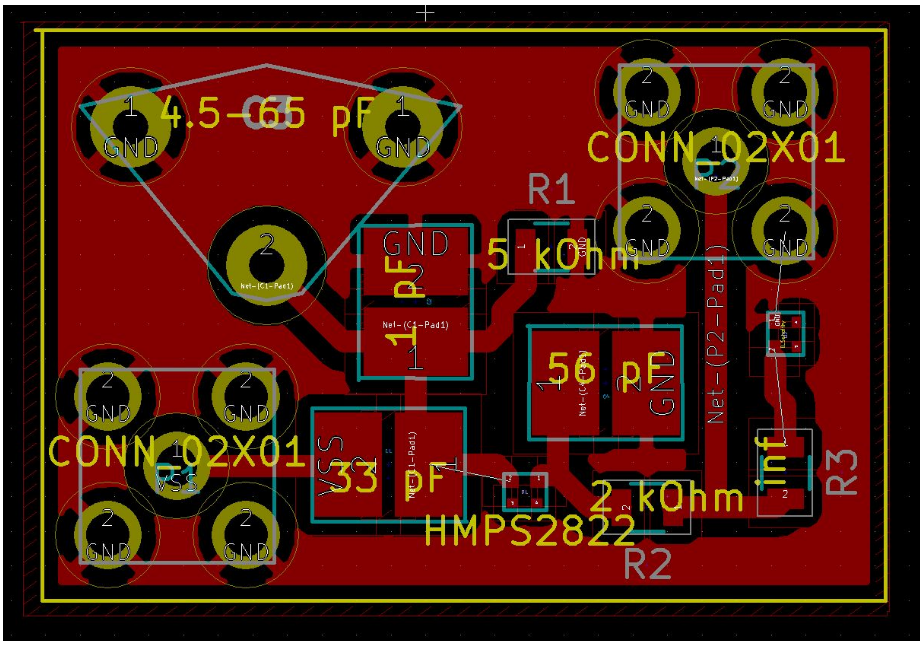


Figure 20: PCB design of the HMPS2822 diode test circuit. Grid size is 1.27 mm. $C_3$, the variable capacitor was removed in the final setup. In $R_3$ no resistor was put (possible resistor for temperature stable setup).

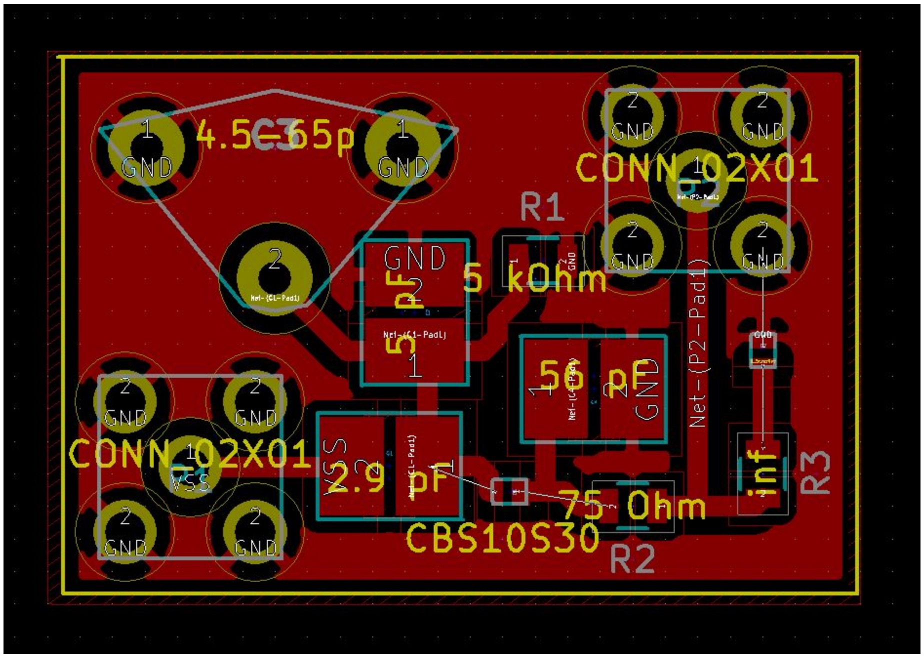


Figure 21: PCB design of the CBS10S30 diode test circuit. Grid size is 1.27 mm. $C_3$, the variable capacitor was removed in the final setup. In $R_3$ no resistor was put (possible resistor for temperature stable setup).

# References

[1] K. G. Johnson et al. "Active stabilization of ion trap radiofrequency potentials". In: *Review of Scientific Instruments* 87.5, 053110 (2016). DOI: `http://dx.doi.org/10.1063/1.4948734`. URL: `http://scitation.aip.org/content/aip/journal/rsi/87/5/10.1063/1.4948734`.

[2] Gandol Davide. "Compact RF Amplifier for Scalable Ion-Traps". PHD-Thesis. UNIVERSITA DEGLI STUDI DI TRENTO Facolta di Scienze Matematiche, Fisiche e Natural, Universität Innsbruck Institut für Experimentalphysik, 2011. URL: `http://www.quantumoptics.at/images/publications/diploma/diplom_gandolfi.pdf` (visited on 11/14/2016).

[3] Florian M. Leupold. "Bang-Bang Control of a Trapped-Ion Oscillator". PHD-Thesis. ETH Zuerich, 2015. URL: `https://www.ethz.ch/content/dam/ethz/special-interest/phys/quantum-electronics/tiqi-dam/documents/phd_theses/thesis_florian_leupold_20160405.pdf` (visited on 12/23/2016).

[4] Thomas P. Harty. "High-Fidelity Microwave-Driven Quantum Logic in Intermediate 43-Ca+". PHD-Thesis. University of Oxford, Department of Physics, 2013, pp. 215–222. URL: `https://www2.physics.ox.ac.uk/`

sites/default/files/2011-08-15/thesisharty_pdf_11742.pdf (visited on 11/14/2016).

[5] Anant Agarwal and Jeffrey H. Lang. *Foundations of analog and digital electronic circuits*. 1st ed. Elsevier, 2005, 214c–214f. ISBN: 1-55860-735-8. URL: http://booksite.elsevier.com/9781558607354/casestudies/04~Chapter_4/Subsection_4_4_1.pdf (visited on 10/21/2016).

[6] *Diode Detector*. URL: http://analog.intgckts.com/rf-power-detector/diode-detector-2/ (visited on 10/29/2016).

[7] O.A. Palusinski. *Session 4 - Computer Aided Engineering for Integrated Circuits. Diode Models*. University of Arizona Department of Electrical and Computer Engineering. 2005. URL: http://www2.engr.arizona.edu/~ece570/session4.pdf (visited on 10/25/2016).

[8] Paul D. Mitcheson. *EE 2.3: Semiconductor Modelling in SPICE. SPICE Diode and BJT models*. Department of Electrical and Electronic Engineering, Imperical College London. URL: http://www3.imperial.ac.uk/pls/portallive/docs/1/7292572.PDF (visited on 10/25/2016).

[9] William Shockley. "The Theory of p-n Jubctions in Semiconductors and p-n Junction Transistors". In: *The Bell System technical journal* 28 (1922), pp. 435–490. URL: https://ia902707.us.archive.org/15/items/bellsystemtechni28amerrich/bellsystemtechni28amerrich.pdf (visited on 10/21/2016).

[10] *HMPS-282x-Series-Data Sheet*. Avago Technologies. 2003. URL: http://www.avagotech.com/docs/AV02-0571EN (visited on 10/30/2016).

[11] *The Zero Bias Schottky Diode Detector at Temperature Extermes - Problems and Solutions. Application Note 1090*. Agilent Technologies. 1999. URL: http://cp.literature.agilent.com/litweb/pdf/5966-0784E.pdf (visited on 10/30/2016).

[12] *CBS10S30*. Toshiba. 2014. URL: https://toshiba.semicon-storage.com/info/docget.jsp?did=14076&prodName=CBS10S30 (visited on 10/31/2016).

[13] R. Williams. *Modern GaAs Processing Methods*. 2nd ed. Boston: Artech House, 1990.

[14] Kent Walters and Bob Werner. *Introduction to Schottky Rectifiers*. Microsemi Corporate Applications. URL: http://www.microsemi.com/document-portal/doc_view/14630-introduction-to-schottky-rectifiers (visited on 12/23/2016).